Supplementary materials for

Hepatic stellate cell-derived microfibrillar-associated protein 2 prevents liver fibrosis by regulating extracellular matrix and inflammation

Wen Zhang[1,2,3,#], Wenyue Wu[1,2,3,#], Ning Zhang[1,2,3], Hong Li[2,3,4,5], Yameng Sun[1,2,3,6], Xiaodong Ge[7], Hui Han[7], Shuyan Chen[1,2,3], Anjian Xu[2,3,4,5], Sai Santosh Babu Komakula[7], Chao Wang[7], Nithyananthan Subramaniyam[7], Qi Han[1,2,3], Aiting Yang[2,3,4,5], Xuzhen Yan[2,3,4,5], Natalia Nieto[7,8,9,*], Hong You[1,2,3,9,*], Wei Chen[2,3,4,5,6,7,*]

[1] Liver Research Center, Beijing Friendship Hospital, Capital Medical University, Beijing 100050, China.

[2] State Key Lab of Digestive Health, Beijing Friendship Hospital, Capital Medical University, Beijing 100050, China.

[3] National Clinical Research Center of Digestive Diseases, Beijing Friendship Hospital, Capital Medical University, Beijing 100050, China.

[4] Experimental and Translational Research Center, Beijing Friendship Hospital, Capital Medical University, Beijing 100050, China.

[5] Beijing Clinical Research Institute, Beijing Friendship Hospital, Capital Medical University, Beijing 100050, China.

[6] Chinese Institutes for Medical Research (CIMR), Beijing 10069, China.

[7] Department of Pathology, University of Illinois Chicago, Chicago, IL 60612, USA.

[8] Division of Gastroenterology and Hepatology, Department of Medicine, University of Illinois Chicago, Chicago, IL 60612, USA.

[9] Authors share co-senior authorship.

[#]These authors contributed equally.

[*]**Corresponding Authors:**

Wei Chen, Experimental and Translational Research Center, Beijing Friendship Hospital, Capital Medical University, No. 95 Yong'an Road, Xicheng District, Beijing 100050, China. E-mail: cw_2011@126.com. Tel: +86 (010) 6313-9311

Hong You, Liver Research Center, Beijing Friendship Hospital, Capital Medical University, No. 95 Yong'an Road, Xicheng District, Beijing 100050, China. E-mail: youhong30@sina.com. Tel: +86 (010) 6313-9019

Natalia Nieto, Division of Gastroenterology and Hepatology, Department of Medicine, University of Illinois Chicago, 840 S. Wood St., Suite 130 CSN, MC 847, Chicago, IL 60612, USA. E-mail: nnieto@uic.edu. Tel: +1 (312) 996-7316

Running title: MFAP-2 alleviates liver fibrosis.

1. **Supplementary figures**
2. **Supplementary tables**

Supplementary figures

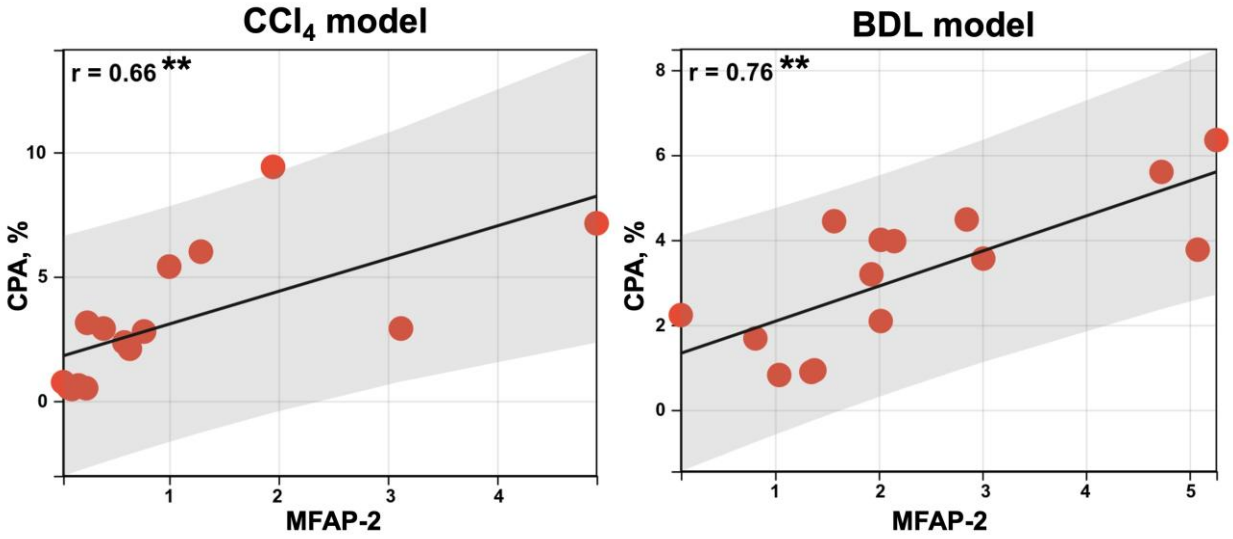

Figure S1. Correlation of liver MFAP-2 protein expression with fibrogenesis. The Pearson correlation analysis between MFAP-2 protein expression and CPA in the CCl_4 and BDL mouse models. $^{**}p < 0.01$. CPA, collagen proportional area.

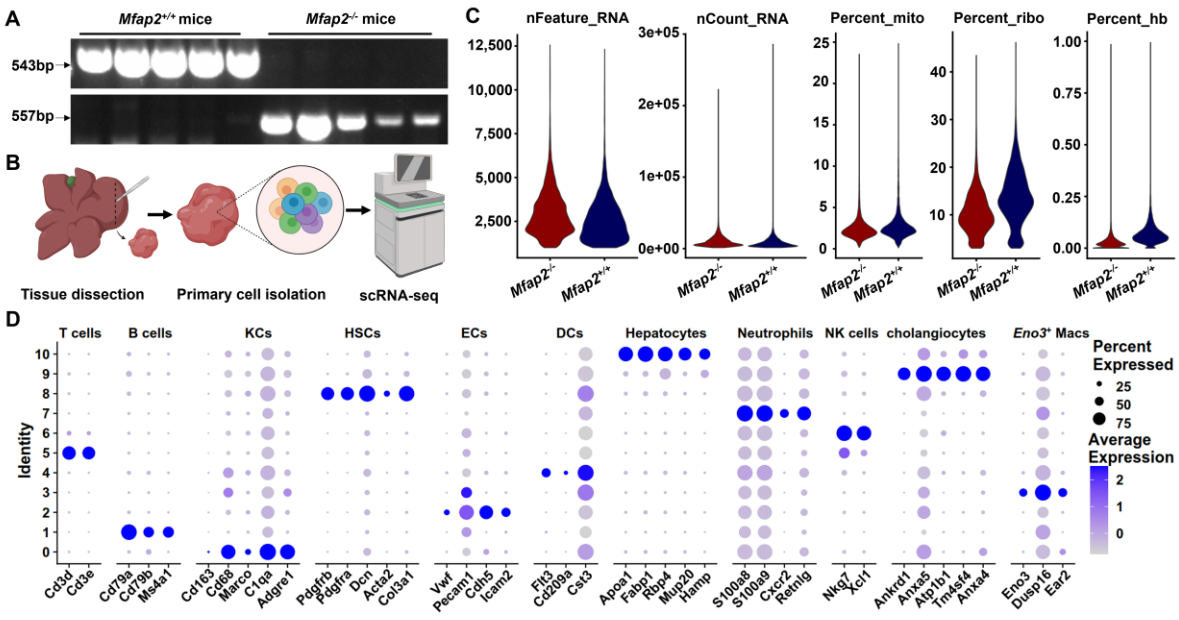

Figure S2. scRNA-seq workflow and data preprocessing. (**A**) Genotyping results show bands for *Mfap2*$^{+/+}$ alleles (543 bp) and *Mfap2*$^{-/-}$ alleles (557 bp). (**B**) Schematic representation of the cell preparation and scRNA-seq workflow. (**C**) Violin plots displaying the distribution of gene counts (nFeature_RNA), UMIs (nCount_RNA), and the

percentages of mitochondrial (percent_mito), ribosomal (percent_ribo), and hemoglobin (percent_hb) genes in NPCs isolated from *Mfap2*$^{+/+}$ and *Mfap2*$^{-/-}$ mice at eight weeks of CCl_4 injection. (**D**) Dot plot depicting the expression of marker genes for cell type annotation.

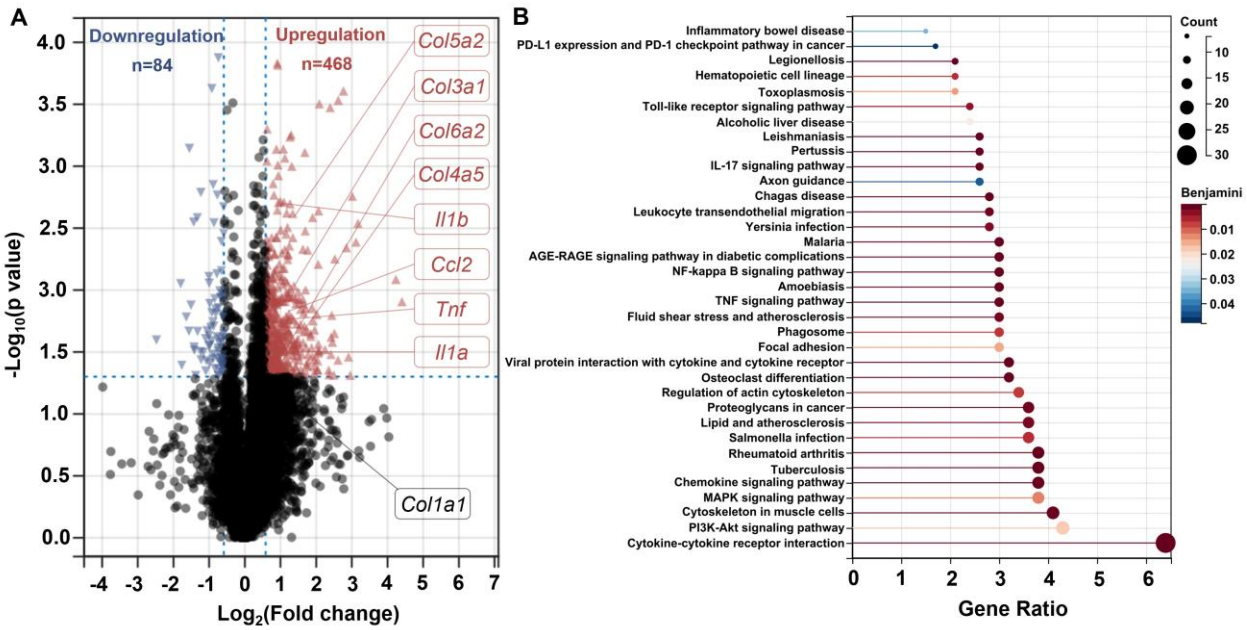

Figure S3. Increased intrahepatic inflammation and activated FA signaling in the livers from *Mfap2*$^{-/-}$ mice following CCl_4 withdrawal. Bulk RNA-seq was conducted on the livers of *Mfap2*$^{-/-}$ and *Mfap2*$^{+/+}$ mice that were administered CCl_4 for eight weeks, followed by a four-week cessation period. (**A**) The volcano plot displays differentially expressed genes (n = 4 per group; $p < 0.05$ & fold change > 1.5). (B) Significantly enriched KEGG pathways derived from upregulated genes (Benjamini-corrected $p < 0.05$).

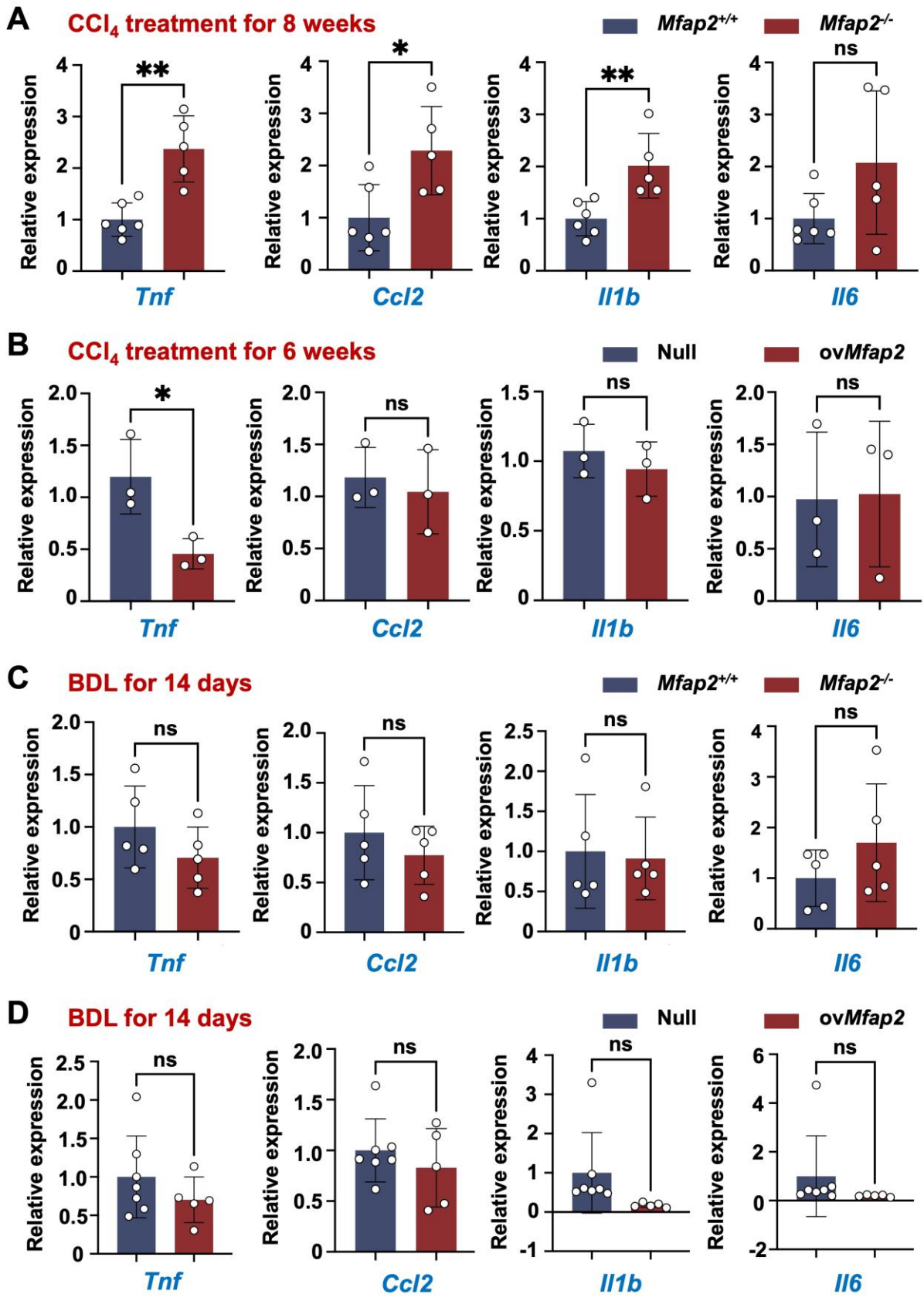
A
CCl4 treatment for 8 weeks
Mfap2+/+
Mfap2-/-
Relative expression
Tnf
Ccl2
Il1b
Il6
**
*
**
ns
B
CCl4 treatment for 6 weeks
Null
ovMfap2
*
ns
ns
ns
C
BDL for 14 days
Mfap2+/+
Mfap2-/-
ns
ns
ns
ns
D
BDL for 14 days
Null
ovMfap2
ns
ns
ns
ns

75

Figure S4. qPCR analysis of pro-inflammatory gene expression. Gene expression of liver *Tnf*, *Ccl2*, *Il1b*, or *Il6* was compared between (**A**) *Mfap2*$^{-/-}$ and *Mfap2*$^{+/+}$ mice at eight weeks of CCl_4 injection (n = 5-6/group), (**B**) Null and ov*Mfap2* mice at six weeks of CCl_4 injection (n = 3/group), (**C**) *Mfap2*$^{-/-}$ and *Mfap2*$^{+/+}$ mice after BDL operation (n = 5/group), or (**D**) Null and ov*Mfap2* mice after BDL operation (n = 5-7/group). Data are expressed as mean ± SEM. *p < 0.05; **p < 0.01; ns, not significant.

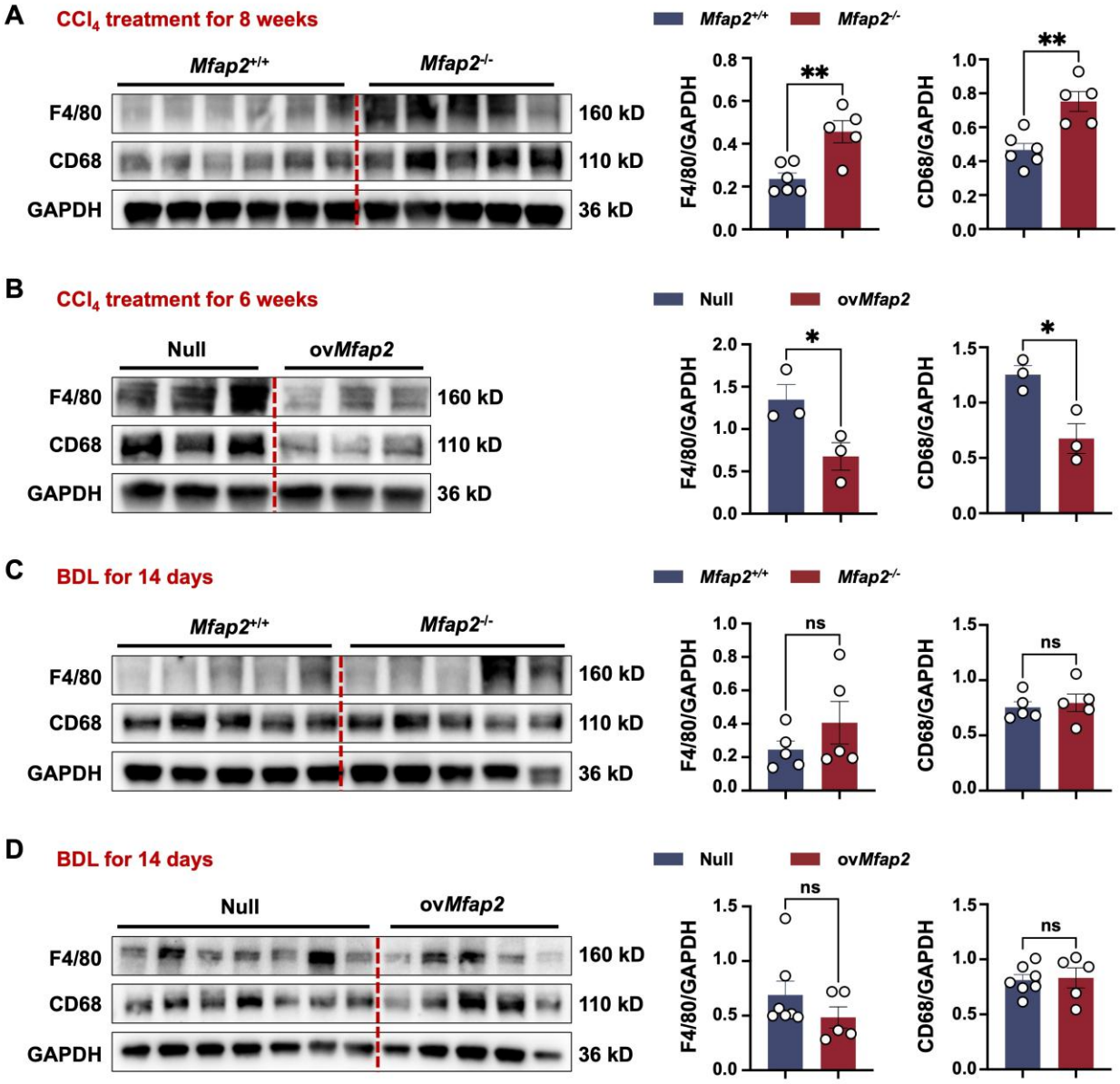

Figure S5. MFAP-2 mitigates liver inflammation in CCl_4 but not BDL mouse liver fibrosis models. Immunoblotting analysis was conducted to compare the expression of

F4/80 and CD68 proteins in liver tissues from (**A**) *Mfap2*$^{+/+}$ and *Mfap2*$^{-/-}$ mice subjected to 8 weeks of CCl_4 treatment (n = 5-6/group), (**B**) Null and ov*Mfap2* mice after 6 weeks of CCl_4 treatment (n = 3/group), and (**C**) *Mfap2*$^{+/+}$ and *Mfap2*$^{-/-}$ mice following BDL (n = 5/group), as well as (**D**) Null and ov*Mfap2* mice post-BDL (n = 5-7/group). Data are presented as mean ± SEM. *$p < 0.05$, **$p < 0.01$; ns, not significant.

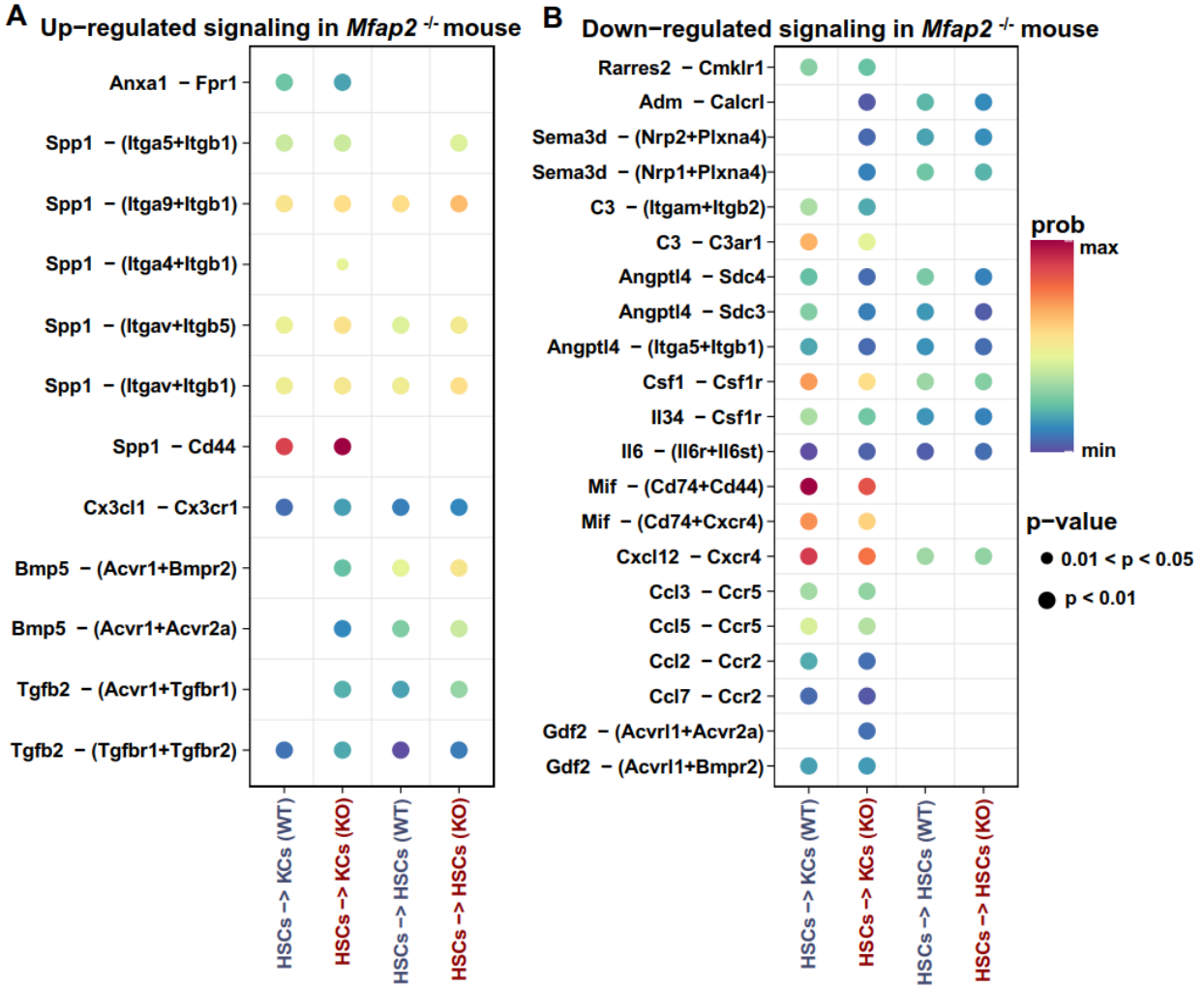

Figure S6. Alterations in signaling dynamics from HSCs to HSCs or liver-resident Møs (Kupffer cells, KCs) following *Mfap2* ablation in CCl_4-injected mice. Upregulated and downregulated signaling pathways are illustrated by comparing the communication probabilities mediated by ligand-receptor pairs from HSCs to HSCs or KCs in *Mfap2*$^{-/-}$ compared to *Mfap2*$^{+/+}$ mice at eight weeks of CCl_4 injection. The dot color

and size represent the calculated communication probability and the statistical significance, respectively.

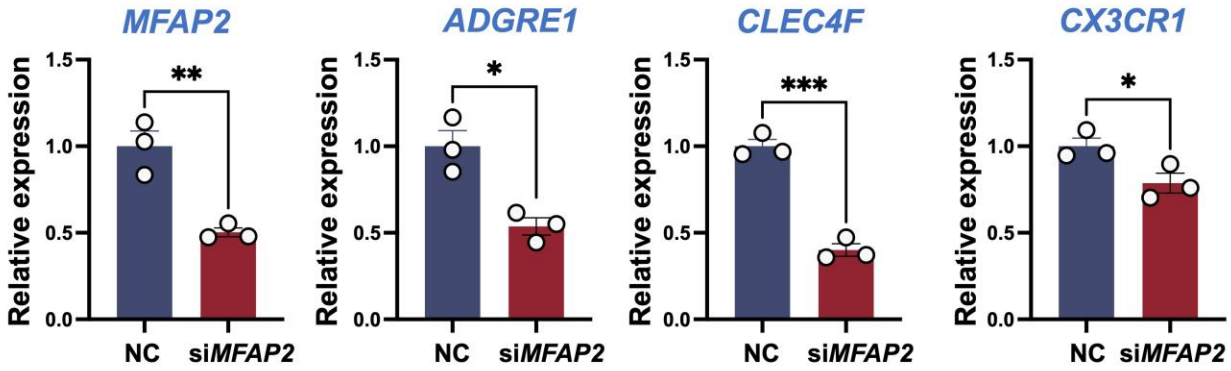

Figure S7. Silencing of *MFAP2* inhibits the activation of Møs. qPCR analysis of *MFAP2*, *ADGRE1*, *CLEC4F*, or *CX3CR1* gene expression in THP-1 cells with si*MFAP2* treatment (n = 3/group, 50 nM, 24 hours). Data are expressed as mean ± SEM. **p* < 0.05, ***p* < 0.01, ****p* < 0.001. NC, negative control.

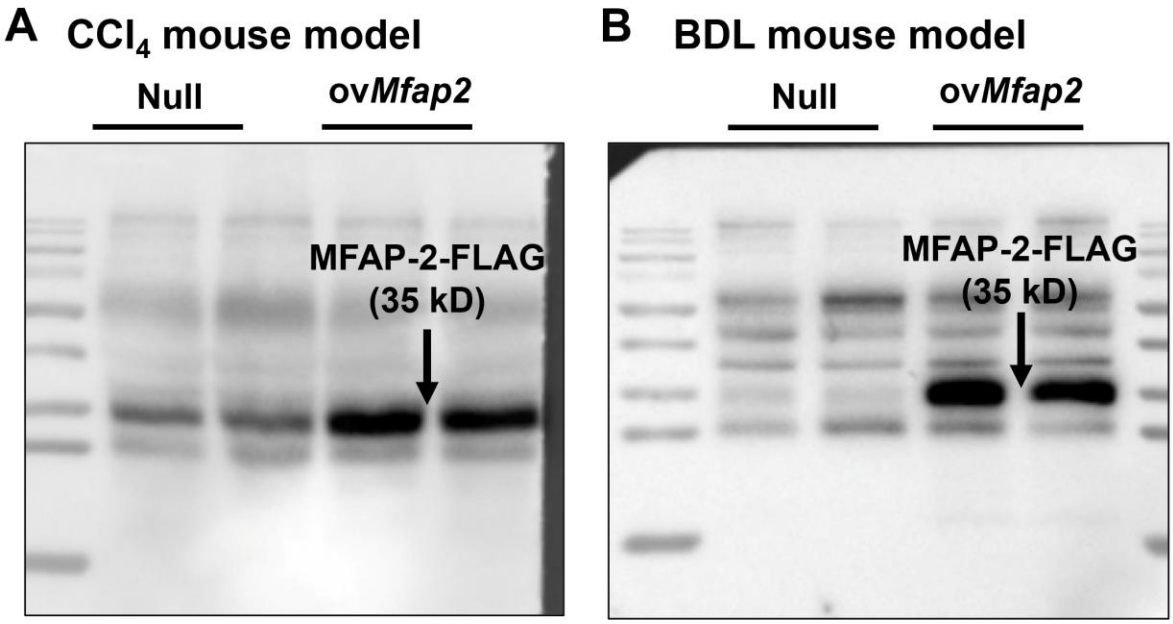

Figure S8. Verification of ov*Mfap2* expression efficiency in mice. Representative bands of immunoblotting analysis of liver FLAG expression in ov*Mfap2* mice injected intravenously with AAV6-CMV-*Mfap2*-HA-EF1a-mNeonGreen-3×FLAG-WPRE vector

and their controls (AAV6-CMV-MCS-EF1a-mNeonGreen-3×FLAG-WPRE vector, Null) in both the (**A**) CCl_4 and (**B**) BDL mouse models (n = 2/group).

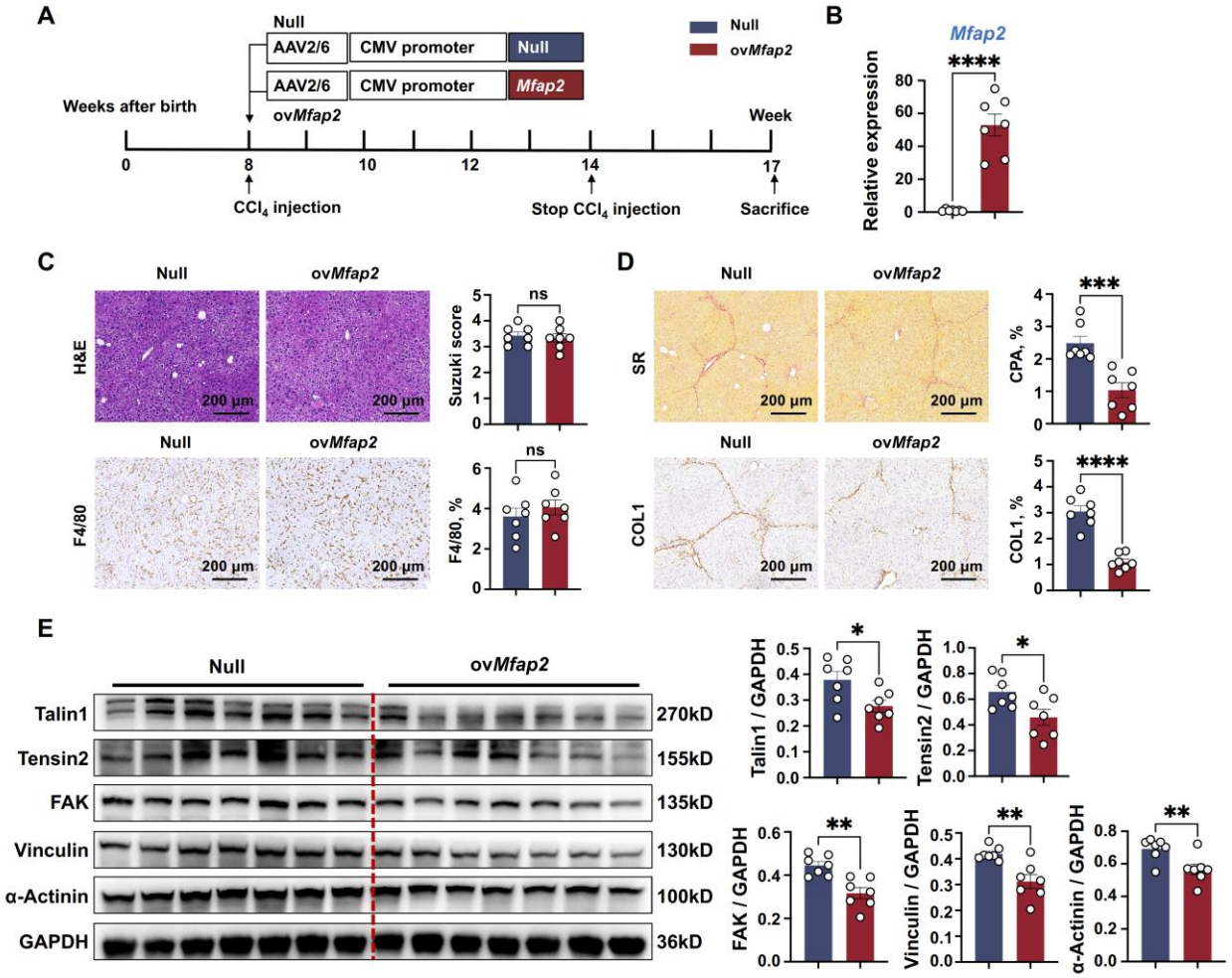

Figure S9. Ov*Mfap2* in HSCs facilitates liver fibrosis regression after CCl_4 cessation for three weeks. (**A**) Schematic diagram illustrating the model of CCl_4-induced liver fibrosis and subsequent resolution. (**B**) qPCR analysis of *Mfap2* gene expression (n = 7/group). (**C**) H&E staining of liver slices and IHC analysis of F4/80 expression (n = 7/group). (**D**) Sirius Red staining of liver sections and IHC analysis of COL1 expression (n = 7/group). (**E**) Immunoblotting analysis of FA signaling markers (n = 7/group). Data are expressed as mean ± SEM. *p < 0.05, **p < 0.01, ***p < 0.001, ****p < 0.0001.

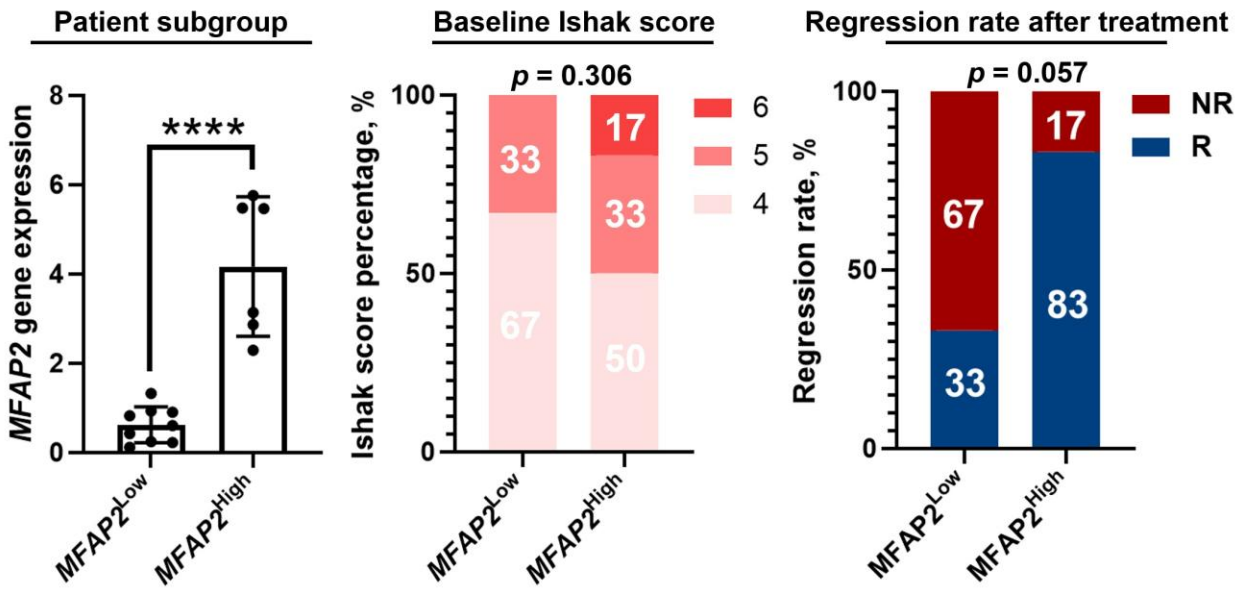

Figure S10. Patients with significant liver fibrosis and elevated baseline *MFAP2* expression are more likely to experience fibrosis regression following etiology control. A total of 15 liver transcriptomic profiles from patients with a baseline Ishak score of ≥ 4 were included in the analysis. Patients were divided into two subgroups based on baseline *MFAP2* gene expression levels: *MFAP2*^{Low} (FPKM < 2, n = 9) and *MFAP2*^{High} (FPKM > 2, n = 6). The baseline Ishak score and the rate of regression were compared between the two patient groups using Chi-square trend test and Chi-square test. Continuous data are presented as mean ± SEM, while categorical data are expressed as percentages. ****p < 0.0001.

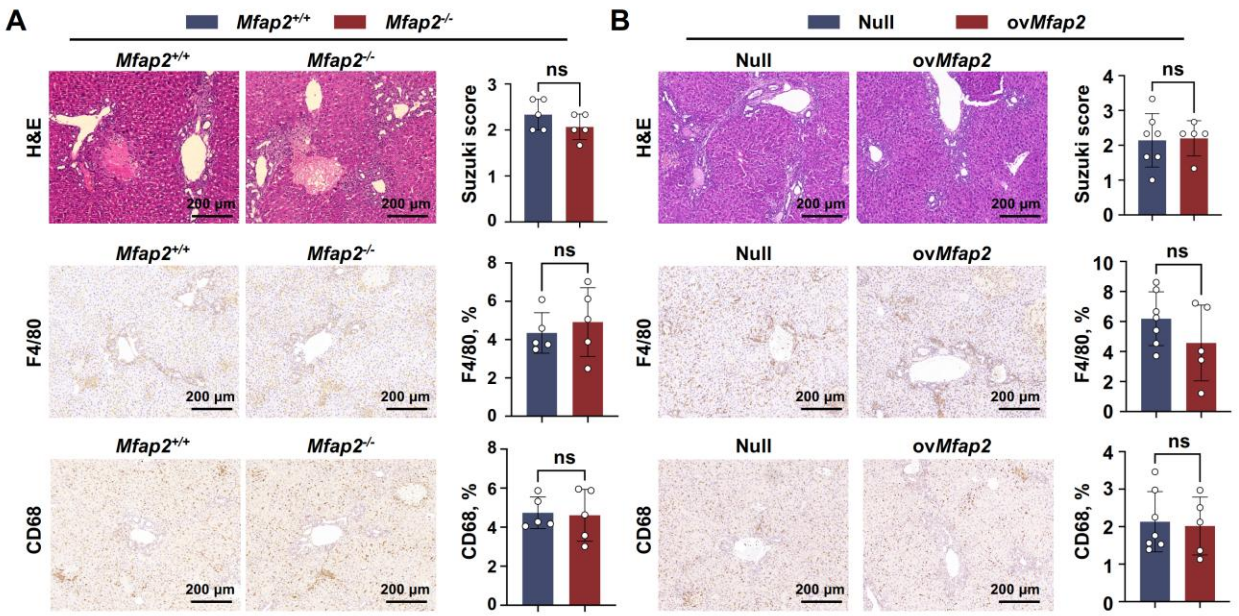

Figure S11. H&E staining and immunostaining analysis of F4/80 or CD68. The Suzuki score based on H&E staining and the percentage of F4/80^{+} and CD68^{+} cells were calculated and compared between (**A**) *Mfap2*$^{+/+}$ and *Mfap2*$^{-/-}$ mice (n = 5/group), or (**B**) Null and ov*Mfap2* mice (n = 5-7/group) post-BDL. Data are expressed as mean ± SEM. ns, not significant.

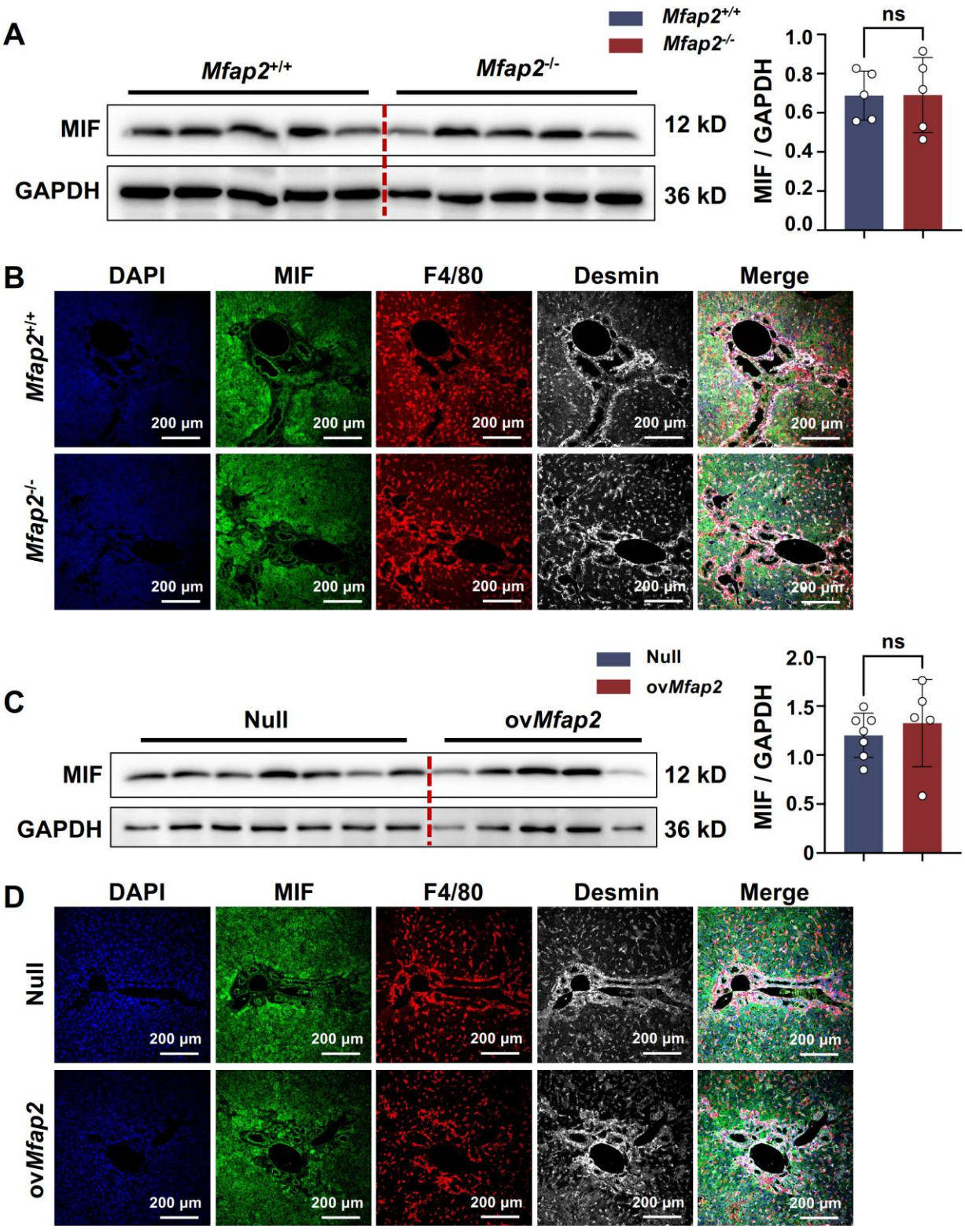

155 **Figure S12. Effects of *Mfap2* ablation or ov*Mfap2* on liver MIF expression in BDL**
156 **mouse models.** (**A, C**) Immunoblotting analysis of MIF in total livers of *Mfap2*$^{-/-}$, *Mfap2*$^{+/+}$,
157 ov*Mfap2,* or Null mice post-BDL (n = 5-7/group). (**B, D**) Multiplex IF staining of MIF (green),

Desmin (red), F4/80 (blue), and DAPI (nucleus, grey) in liver slices of *Mfap2*$^{-/-}$, *Mfap2*$^{+/+}$, ov*Mfap2* or Null mice post-BDL. The merged areas of MIF and Desmin are indicated in yellow. Data are expressed as mean ± SEM. ns, not significant.

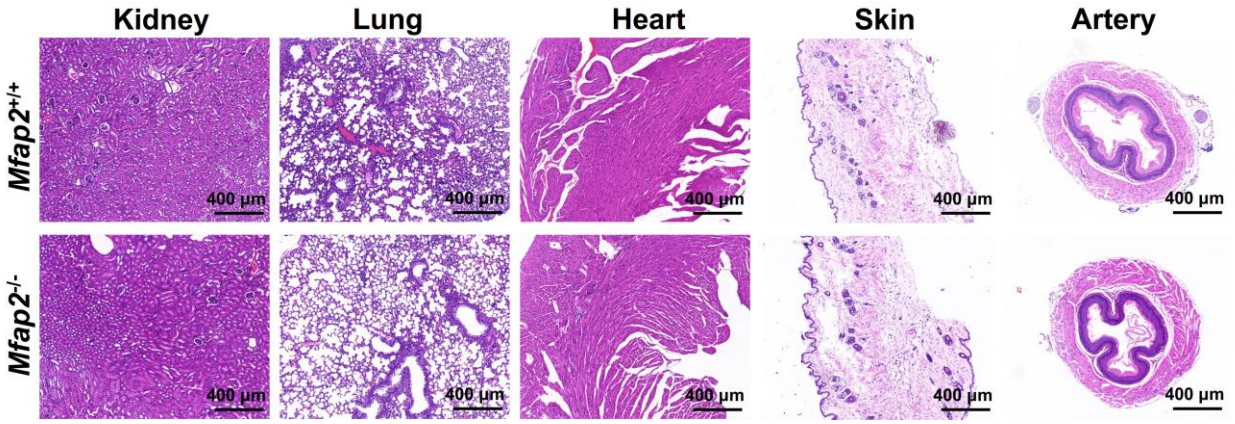

Figure S13. Effects of *Mfap2* deletion on the structure of elastin-rich tissues. H&E staining of kidney, lung, heart, skin, and artery sections from *Mfap2*$^{+/+}$ and *Mfap2*$^{-/-}$ mice.

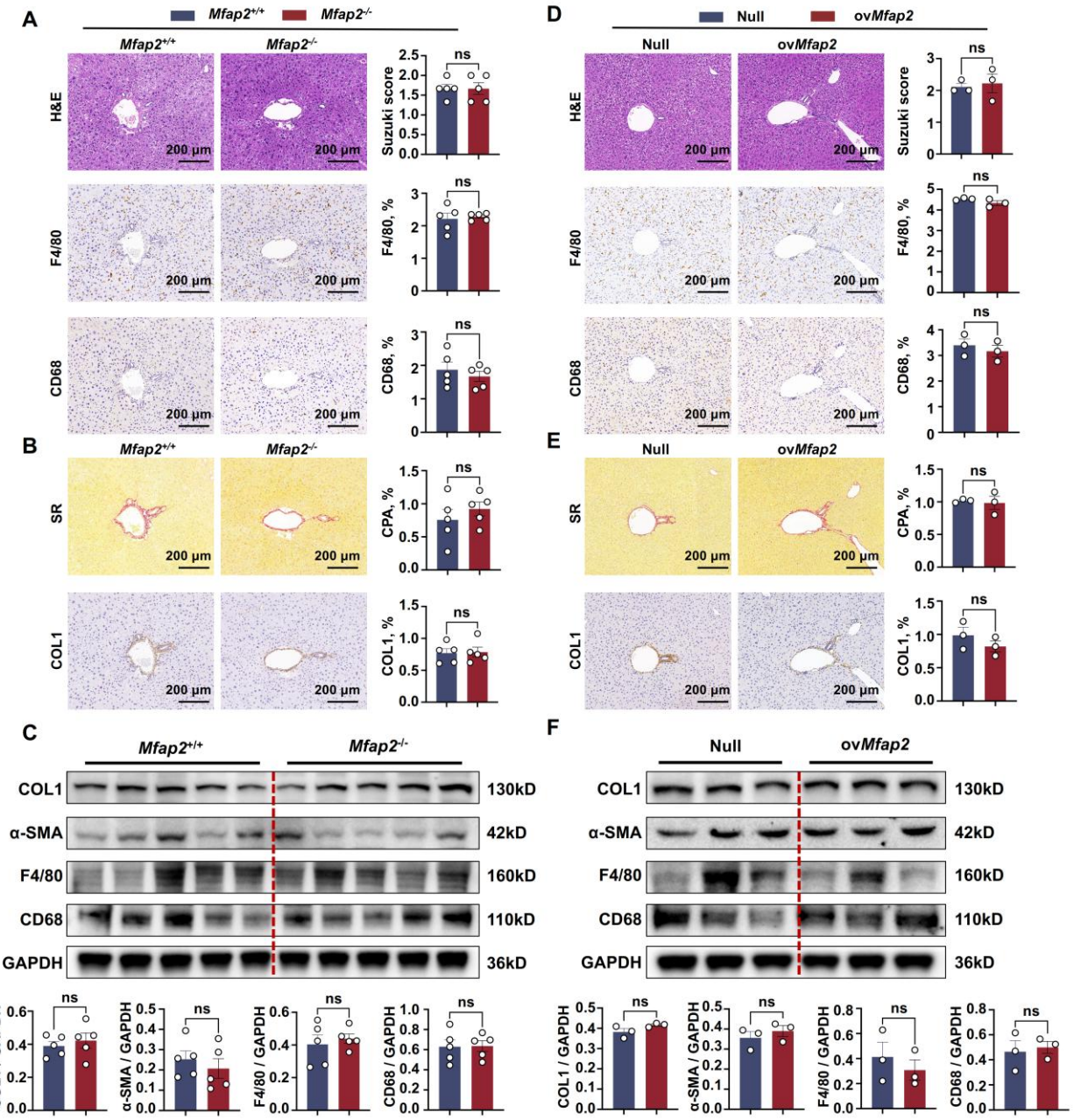

165 **Figure S14. Effects of *Mfap2* intervention on mouse livers in the absence of**
166 **intoxication.** H&E staining and Sirius Red staining of liver sections, along with IHC
167 analysis of F4/80, CD68, and COL1 expression, were performed. Additionally,
168 immunoblotting was conducted to evaluate the protein expression levels of COL1, α-SMA,
169 F4/80, and CD68. Comparisons were made between MO-injected *Mfap2*$^{+/+}$ and *Mfap2*$^{-/-}$
170 mice (n = 5/group) in panels **A-C**, and between MO-injected Null and ov*Mfap2* mice (n =
171 3/group) in panels **D-F**.
172

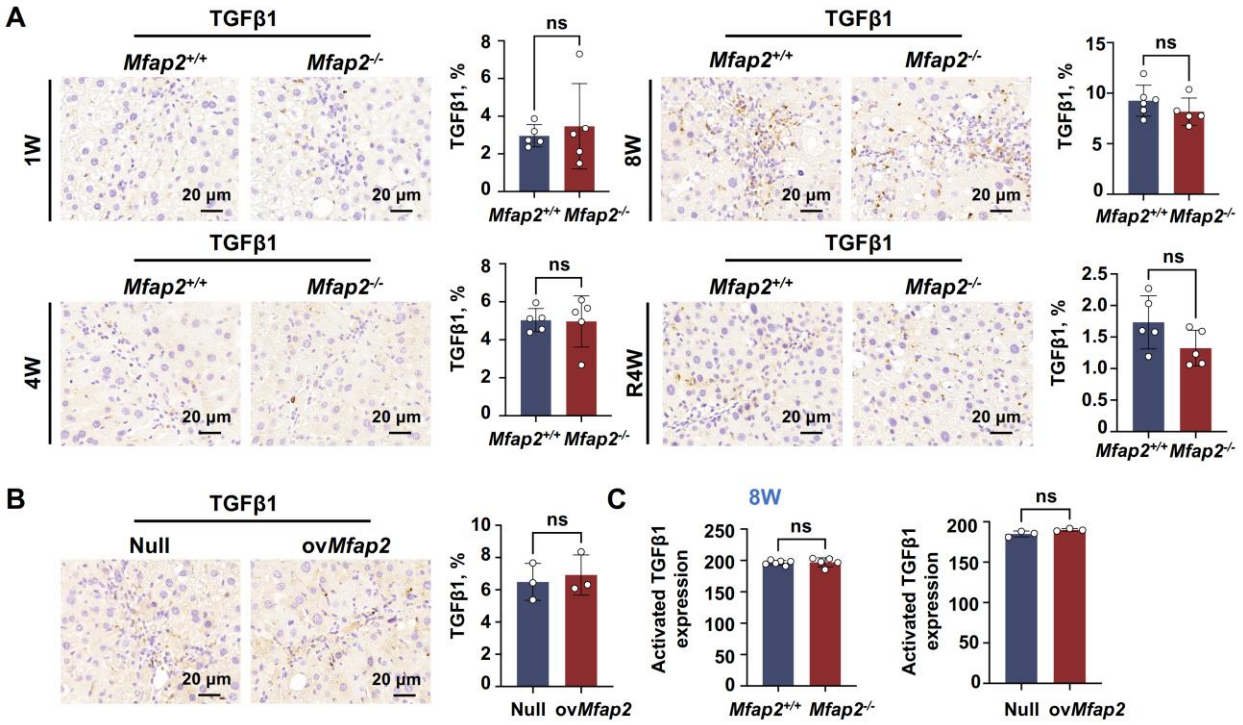

173 **Figure S15. Effects of *Mfap2* deletion or ov*Mfap2* on intrahepatic TGFβ1 expression.**
174 (**A**) Immunostaining analysis of TGFβ1 in liver sections between *Mfap2*$^{+/+}$ and *Mfap2*$^{-/-}$
175 mice after one (1W), four (4W), or eight (8W) weeks of CCl_4 injection, as well as four
176 weeks after CCl_4 cessation (R4W) (n = 5-6/group). (**B**) Immunostaining analysis of TGFβ1
177 in liver sections between ov*Mfap2* and Null mice after six weeks of CCl_4 injection (n =
178 3/group). (**C**) Comparison of activated TGFβ1 levels between *Mfap2*$^{+/+}$ and *Mfap2*$^{-/-}$ mice
179 after eight weeks (8W) of CCl_4 injection (n = 5-6/group) or between ov*Mfap2* and Null
180 mice after six weeks of CCl_4 injection (n = 3/group). Data are expressed as mean ± SEM.
181 ns, not significant.

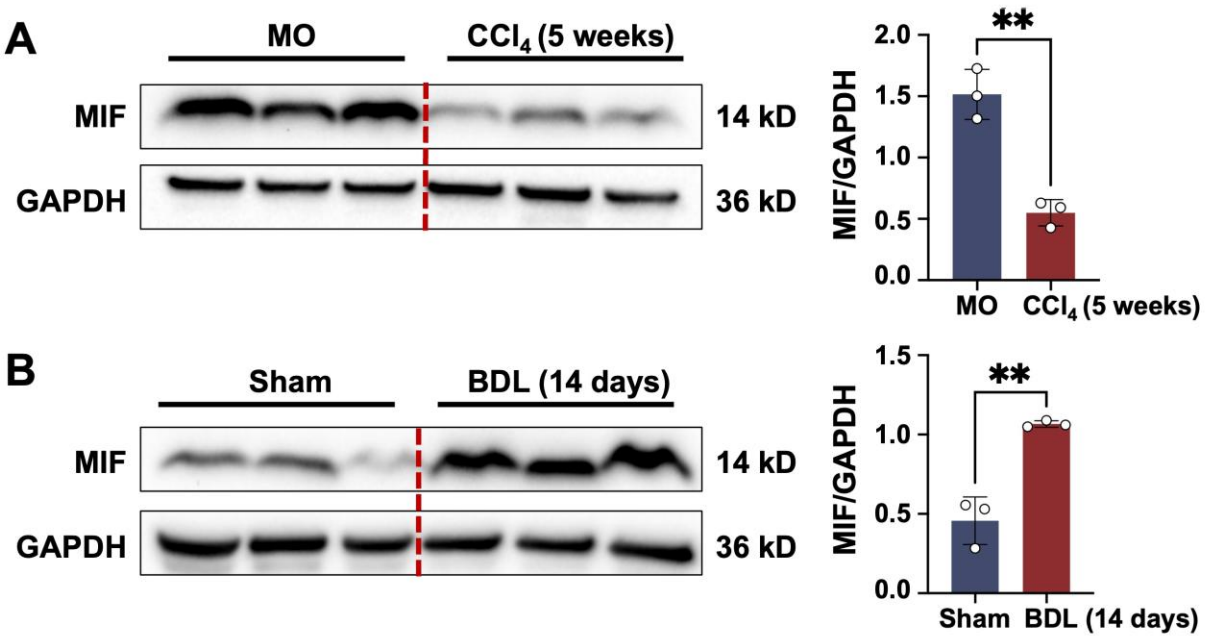

182 **Figure S16. Liver MIF expression in experimental liver fibrogenesis.** Immunoblotting
183 analysis of liver MIF in (**A**) CCl_4 (six weeks) or (**B**) BDL (fourteen days) mouse models (n
184 = 3/group). Data are expressed as mean ± SEM. ***p* < 0.01.
185

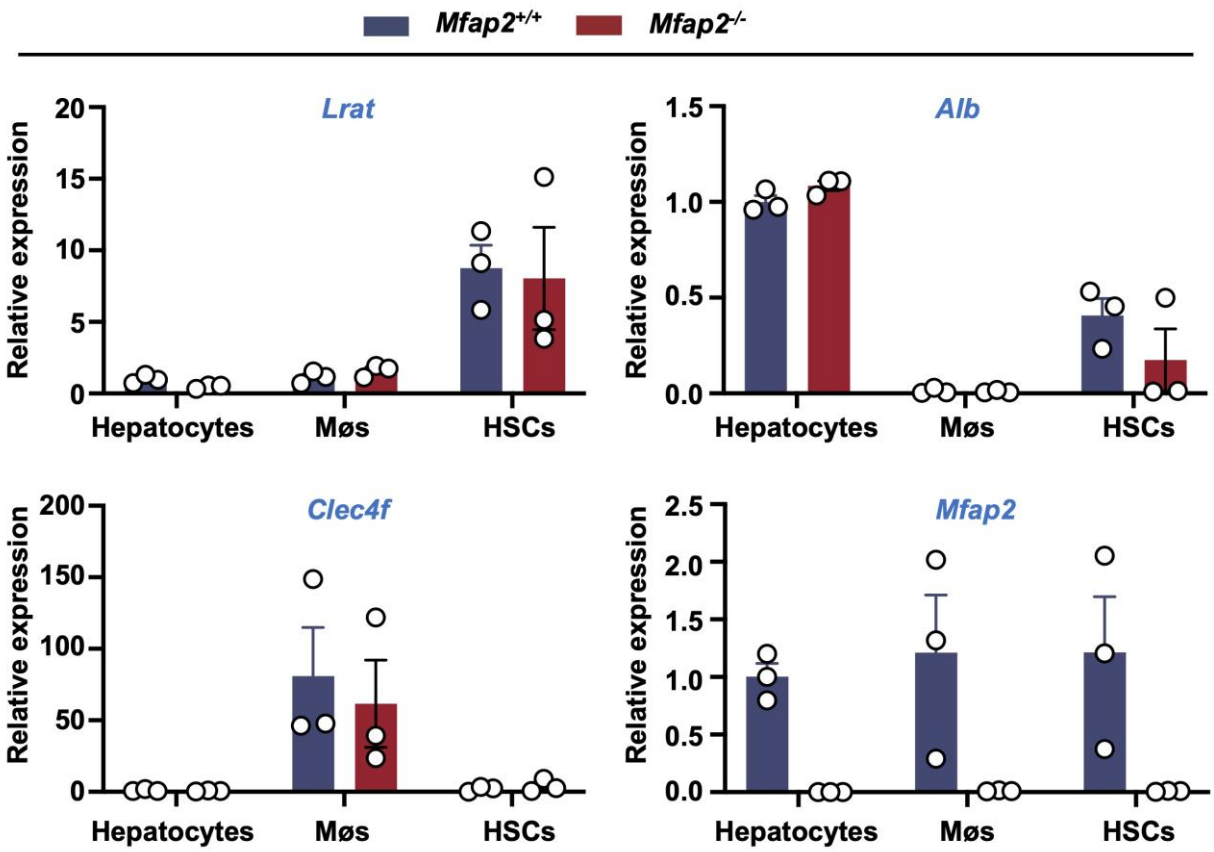

Figure S17. *Mfap2* gene expression in primary liver cells from normal *Mfap2*$^{+/+}$ and *Mfap2*$^{-/-}$ mice. qPCR was conducted to assess the expression levels of *Lrat*, *Alb*, *Clec4f*, and *Mfap2* genes in primary HSCs, hepatocytes, and Møs isolated from both *Mfap2*$^{+/+}$ and *Mfap2*$^{-/-}$ mice without any treatment (n = 3/group, male, 10-month-old). Data are expressed as mean ± SEM.

Supplementary tables

Table S1. Publicly available gene expression profiles of liver fibrosis from the GEO database used in this study.

GEO ID	Etiology	Sample size	Sample resource	Platform	Year
GSE84044	HBV	F0 = 43 F1 = 20 F2 = 33 F3 = 18 F4 = 10	Frozen liver biopsy	GPL570	2016
GSE149601	HCV	Non-LC = 140 LC = 55	Liver biopsy	GPL20301	2020
GSE193066	MASLD	F0-1 = 51 F2 = 71 F3-4 = 43	Liver biopsy	GPL18573	2022
GSE55747	CCl_4	Con = 4 CCl4 = 6	unknown	GPL6885	2017
GSE74605	TAA	Con = 3 TAA = 3	unknown	GPL6885	2015
GSE145086	CCl_4	Control = 3 CCl_4 2 weeks = 3 CCl_4 4 weeks = 3	NPCs	GPL24247	2020
GSE233751	CCl_4	MO = 3 Liver fibrosis = 3 Resolution = 3	NPCs	GPL24247	2024

GEO: Gene Expression Omnibus; HBV: hepatitis B virus; HCV: hepatitis C virus; LC: liver cirrhosis; MO: mineral oil; non-LC: non-liver cirrhosis; NPCs: non-parenchymal cells; TAA: thioacetamide.

Table S2. List of resources used in this study.

Reagent or resource	Source	Identifier
Antibodies		
Anti-CD34 (application: IF/ICC; dilution: 1:100)	Abcam	Cat#ab81289
Anti-CD68 (application: IHC/WB; dilution: 1:100/1:1000)	Thermo Fisher Scientific	Cat#PA5-78996
Anti-COL1 (application: IHC/IF; dilution: 1:100)	CST	Cat#72026
Anti-COL1 (application: WB; dilution: 1:1000)	Thermo Fisher Scientific	Cat#PA5-95137
Anti-COL1 (A2) (application: IF; dilution: 1:100)	Santa Cruz	Cat#sc-393573
Anti-COL3 (application: IF; dilution: 1:100)	Abcam	Cat#ab7778
Anti-Desmin (application: mIF; dilution: 1:500)	Thermo Fisher Scientific	Cat#MA5-32068
Anti-Elastin (application: IF; dilution: 1:100)	Millipore	Cat#MAB2503
Anti-F4/80 (application: IF; dilution: 1:100)	Abcam	Cat#ab6640
Anti-F4/80 (application: mIF/IHC/WB; dilution: 1:100/1:1000)	CST	Cat#70076
Anti-FAK (application: WB; dilution: 1:1000)	CST	Cat#3285
Anti-FBLN-1 (application: IF/WB; dilution: 1:100/1:1000)	ABclonal	Cat#A16677
Anti-FLAG (application: WB; dilution: 1:1000)	Medical & Biological Laboratories	Cat#M185-3L
Anti-GAPDH (application: WB; dilution: 1:10000)	Abcam	Cat#ab8245
Anti-LOXL1 (application: IF; dilution: 1:100)	Santa Cruz	Cat#sc-166632
Anti-LOXL1 (application: WB; dilution: 1:1000)	Thermo Fisher Scientific	Cat#PA5-87701
Anti-LYVE1 (application: IF; dilution: 1:100)	Abcam	Cat#ab281587
Anti-MAGP1 (application: IF; dilution: 1:50)	Santa Cruz	Cat#sc-166075

Anti-MAGP1 (application: IHC; dilution: 1:200)	Novus	Cat#NBP1-87735
Anti-MIF (application: WB/IHC; dilution: 1:1000/1:100)	CST	Cat#87501
Anti-Talin-1 (application: WB/mIF; dilution: 1:1000)	CST	Cat#4021
Anti-Tensin-2 (application: WB; dilution: 1:1000)	CST	Cat#11990
Anti- TGFβ1 (application: IHC; dilution: 1:1000)	Thermo Fisher Scientific	Cat#MA-21595
Anti-Vinculin (application: WB; dilution: 1:1000)	CST	Cat#4650
Anti-α-Actinin (application: WB; dilution: 1:1000)	CST	Cat#6487
Anti-α-SMA (application: IF/mIF; dilution: 1:100)	Abcam	Cat#ab7817
Anti-α-SMA (application: WB; dilution: 1:1000)	Abcam	Cat#ab5694
Alexa Fluor 488 donkey anti-rabbit IgG(H+L) (application: secondary antibody; dilution: 1:500)	Invitrogen	Cat#A21206
Alexa Fluor 488 donkey anti-mouse IgG(H+L) (application: secondary antibody; dilution: 1:500)	Invitrogen	Cat#A21202
Alexa Fluor 594 donkey anti-rabbit IgG(H+L) (application: secondary antibody; dilution: 1:500)	Invitrogen	Cat#A21207
Alexa Fluor 594 donkey anti-mouse IgG(H+L) (application: secondary antibody; dilution: 1:500)	Invitrogen	Cat#A21203
Alexa Fluor 594 donkey anti-rat IgG(H+L) (application: secondary antibody; dilution: 1:500)	Invitrogen	Cat#A21209
Anti-mouse IgG HRP-linked Ab (application: secondary antibody; dilution: 1:5000)	ZSGB-Bio	Cat#ZB-2305

Anti-rabbit IgG HRP-linked Ab (application: secondary antibody; dilution: 1:5000)	ZSGB-Bio	Cat#ZB-2301
Chemicals, peptides, commercial kits, and recombinant proteins		
4',6-diamidino-2-phenylindole	Abcam	Cat#ab104139
Acetone	Sinopharm Chemical Reagent Co., Ltd	Cat#10000418
Acetonitrile	Sigma	Cat#34851
Agilent High Sensitivity DNA Kit	Agilent	Cat#5067-4626
Alanine Aminotransferase Assay Kit	Nanjing Jiancheng	Cat# C009-2-1
Ammonium bicarbonate	Sigma	Cat#09830
Aspartate Aminotransferase Assay Kit	Nanjing Jiancheng	Cat# C010-2-1
Carbon tetrachloride	Innochem	Cat#A68354
Chromium Single Cell 3' Library & Single Cell 3' v3 Gel Beads	10× Genomics	Cat#PN-1000075
Citrate buffer	ZSGB-BIO	Cat#ZLI-9064
DAB HRP Substrate Kit	ZSGB-BIO	Cat#ZLI-9018
Dithiothreitol	Thermo Fisher Scientific	Cat#20290
DynaBeads® MyOneTM Silane Beads	Life Technologies	Cat#37002D
Fast Mouse Genotyping Kit	Beyotime	Cat#D7283S
Fetal bovine serum	Sigma	Cat#F8687-500ml
Formic acid	Sigma	Cat#27001
H&E Staining Kit	Solarbio	Cat# G1120
Human liver tissue array	US Biomax, Inc	Cat# LV805b

Hydrogen peroxide (3%)	Sinopharm Chemical Reagent Co., Ltd	Cat#10011208
Illumina VAHTS® Universal V6 RNA-seq Library Prep Kit	Vazyme	Cat#V6-003
Iodoacetamide	Thermo Fisher Scientific	Cat#ICN10035105
LEGEND MAX™ Free Active TGFβ1 ELISA Kit	Biolegend	Cat# No.437707
Lys-C	Wako	Cat#125-05061
Magnetic oligo (dT) beads	Invitrogen	Cat#61002
Minimum Essential Medium	Procell	Cat#PM150411
Mineral oil	Thermo Fisher Scientific	Cat#J62592.AP
Modified Sirius Red Staining Kit	Solarbio	Cat#G1472
Mouse Liver Dissociation Kit	Miltenyi Biotec	Cat#130-105-807
NaCl	Sigma	Cat#S9888
NEBNext Ultra RNA Library Prep Kit	New England Biolabs	Cat#E7770
Nycodenz	AXELL	Cat#AN1002424
OCT compound	Sakura	Cat#4583
PANO 4-plex IHC kit	Panovue	Cat#TSA-RM-275
Penicillin and streptomycin	Gibco	Cat#15140122
Percoll	Cytiva	Cat#17089109
Pierce BCA Protein Assay Kit	Thermo Fisher Scientific	Cat#23227
Pierce™ Protein Concentrator PES 10K MWCO, 2-6 mL, 24PK	Thermo Fisher Scientific	Cat#88517
PNGaseF	BioLabs	Cat#P0704L
PrimeScript™ RT reagent kit	Takara	Cat#RR037Q
Protease inhibitor	Yeasen	Cat#20124ES03

Qubit dsDNA Assay Kit	Life Technologies	Cat#Q328520
rhTGFβ1	MCE	Cat#HY-P7118
RNA simple Total RNA kit	Fastagen	Cat#220010
RPMI-1640 Complete Medium	Procell	Cat#PM150110B
SDS	Sigma	Cat#L3771
SPRIselect Reagent Kit	Life Technologies	Cat#B23318
Trifluoroacetic acid	Thermo Fisher Scientific	Cat#A116-10X1 AMP
Tris base	Solarbio	Cat#T8060
Triton X-100	Solarbio	Cat#T8200
Trypsin	Promega	Cat#V511A
Urea	Sigma	Cat#U6504
X-tremeGENE HP DNA Transfection Reagent	Roche	Cat#6366236001
Cell lines		
Human: LX-2 cell line	ATCC	N/A
Human: THP-1 cell line	Procell	CL-0233
Organisms/strains		
Mouse: C57BL/6J	HFK Bioscience Co. Ltd.	N/A
Mouse: *Mfap2*$^{-/-}$ and *Mfap2*$^{+/+}$	Cyagen Bioscience Inc.	S-KO-03113
Primers for qPCR and genotyping		
Human_*MFAP2*_forward: 5' – ACCCGCCTCTACTCCATACA – 3' Human_*MFAP2*_reverse: 5' – TAATGACGTACACACGGCGG – 3'	This paper	Designed by Primer-BLAST
Human_*MIF*_forward: 5' – CTGCACAGCATCGGCAAGAT – 3' Human_ *MIF*_reverse: 5' – AGTTGATGTAGACCCTGTCCG – 3'	This paper	Designed by Primer-BLAST

Human_*ADGRE1*_forward: 5’ – CCAGTGTTAATGCCGAAGTCT – 3’ Human_ *ADGRE1*_reverse: 5’ – GTGAACAGGTAAGCCATGACA - 3’	This paper	Designed by Primer-BLAST
Human_*CD163*_forward: 5’ – TTTGTCAACTTGAGTCCCTTCAC – 3’ Human_*CD163*_reverse: 5’ – TCCCGCTACACTTGTTTTCAC – 3’	This paper	Designed by Primer-BLAST
Human_*CLEC4F*_forward: 5’ – CCCCAAGATACCGAGGCTC – 3’ Human_*CLEC4F*_reverse: 5’ – GCCCAGTAATGTTGTCTCCCA – 3’	This paper	Designed by Primer-BLAST
Human_*CX3CR1*_forward: 5’ – ACTTTGAGTACGATGATTTGGCT – 3’ Human_*CX3CR1*_reverse: 5’ – GGTAAATGTCGGTGACACTCTT – 3’	This paper	Designed by Primer-BLAST
Human_*GAPDH*_forward: 5’ – GGAGCGAGATCCCTCCAAAAT – 3’ Human_ *GAPDH*_reverse: 5’ – GGCTGTTGTCATACTTCTCATGG – 3’	This paper	Designed by Primer-BLAST
Mouse_*Alb*_forward: 5’ – TGCTTTTTCCAGGGGTGTGTT – 3’ Mouse_*Alb*_reverse: 5’ – TTACTTCCTGCACTAATTTGGCA – 3’	This paper	Designed by Primer-BLAST
Mouse_*Lrat*_forward: 5’ – CCGTCCCTATGAAATCAGCTC – 3’ Mouse_*Lrat*_reverse: 5’ – ATGGGCGACACGGTTTTCC – 3’	This paper	Designed by Primer-BLAST
Mouse_*Clec4f*_forward: 5’ – GAGGCCGAGCTGAACAGAG – 3’ Mouse_*Clec4f*_reverse:	This paper	Designed by Primer-BLAST

5’ – TGTGAAGCCACCACAAAAAGAG – 3’		
Mouse_*Tnf*_forward: 5’ – GACGTGGAACTGGCAGAAGAG – 3’ Mouse_*Tnf*_reverse: 5’ – TTGGTGGTTTGTGAGTGTGAG – 3’	This paper	Designed by Primer-BLAST
Mouse_*Il1b*_forward: 5’ – GCAACTGTTCCTGAACTCAACT – 3’ Mouse_*Il1b*_reverse: 5’ – ATCTTTTGGGGTCCGTCAACT – 3’	This paper	Designed by Primer-BLAST
Mouse_*Il6*_forward: 5’ – CCAAGAGGTGAGTGCTTCCC – 3’ Mouse_*Il6*_reverse: 5’ – CTGTTGTTCAGACTCTCTCCCT – 3’	This paper	Designed by Primer-BLAST
Mouse_*Ccl2*_forward: 5’ – TTAAAAACCTGGATCGGAACCAA – 3’ Mouse_*Ccl2*_reverse: 5’ – GCATTAGCTTCAGATTTACGGGT – 3’	This paper	Designed by Primer-BLAST
Mouse_*Mfap2*$^{+/+}$_forward: 5’ – TCACCAAGACCACACTCTTGTTA – 3’ Mouse_*Mfap2*$^{+/+}$_reverse: 5’ – CGACCTCTCTAAGAGCCACTTG – 3’	This paper	Cyagen Bioscience Inc.
Mouse_*Mfap2*$^{-/-}$_forward: 5’ – TCACCAAGACCACACTCTTGTTA – 3’ Mouse_*Mfap2*$^{-/-}$_reverse: 5’ – ATTACATAGACCTGTGAGGAGGGAC – 3’	This paper	Cyagen Bioscience Inc.
Mouse_*Mfap2*_forward: 5’ – CGCCGAGTGTATGTGGTCAA – 3’ Mouse_*Mfap2*_reverse: 5’ – ACGCCACACTTGGAgAACTT – 3’	This paper	Designed by Primer-BLAST
Mouse_*Gapdh*_forward: 5’ – TGGCCTTCCGTGTTCCTAC – 3’	This paper	Designed by Primer-BLAST

Mouse_*Gapdh*_reverse: 5’ – GAGTTGCTGTTGAAGTCGCA – 3’		
AAV vectors, plasmids, and siRNAs		
pRP[Exp]-EGFP/Puro-EF1A>hMFAP2/FLAG plasmid	VectorBuilder	Cat#VB230216-1551xdw
pRP[Exp]-EGFP/Puro-EF1A>ORF_Stuffer (null)	VectorBuilder	Cat#VB180929-1003hrg
Human *MFAP2* siRNA Target sequence: ACUGUACGAACACAGAUCUCCTTP	OBiO	Cat#MFAP2-135-A
Negative control siRNA Target sequence: ACGUGACACGUUCGGAGAATT	OBiO	NA
AAV6-CMV-Mfap2-HA-EF1a-mNeonGreen-3×FLAG-WPRE vector	OBiO	Cat#H23692
AAV6-CMV-MCS-EF1a-mNeonGreen-3×FLAG-WPRE vector	OBiO	Cat#H10018
Software		
7500 Software v2.3	Applied Biosystems	https://www.thermofisher.cn/cn/zh/home/brands/applied-biosystems.html
CellChat	Suoqin Jin et al.	https://github.com/sqjin/CellChat
Cufflinks	Cole Trapnell’s lab	http://cole-trapnell-lab.github.io/cufflinks/

DAVID web tool	Brad T Sherman et al.	https://david.ncifcrf.gov/
DoubletFinder v2.0.2	Christopher S McGinnis et al.	https://github.com/chris-mcginnis-ucsf/DoubletFinder
FV10-ASW 4.2 Viewer	Olympus Life Science	https://www.olympus-lifescience.com
Gene Expression Omnibus	National Institutes of Health	https://www.ncbi.nlm.nih.gov/geo/
ggplot2	-	https://cran.r-project.org/web/packages/ggplot2/index.html
GraphPad Prism version 9	Dotmatics	https://www.graphpad.com
HISAT software	Daehwan Kim et al.	https://github.com/infphilo/hisat
ImageJ	the National Institutes of Health	https://imagej.net/ij/
Image Lab Software	Bio-Rad	https://www.bio-rad.com/
Image-Pro Plus software version 6.0	Media Cybernetics	https://image-pro-plus.software.informer.com/6.0/
mMCPcounter	Florent Petitprez et al.	https://github.com/cit-bioinfo/mMCP-counter

Primer-BLAST	National Institutes of Health	https://www.ncbi.nlm.nih.gov/tools/primer-blast
Proteome Discoverer suite version 2.4	Thermo Fisher Scientific	https://www.thermofisher.cn/cn/zh/home.html
ProteomeXchange consortium	Juan A Vizcaíno et al.	https://www.proteomexchange.org/
R 4.2.1	-	https://www.r-project.org/
Rstudio	-	https://posit.co/products/open-source/rstudio/#
Other		

Table S3. Comparison of liver index and blood biochemistry between *Mfap2*$^{+/+}$ and *Mfap2*$^{-/-}$ mice or Null and ov*Mfap2* mice undergoing CCl_4 injection or BDL operation.

	Group	LW/BW ratio	ALT, U/L	AST, U/L
CCl_4 (1W)	***Mfap2*$^{+/+}$**	0.06±0.00	95.16±13.66	33.86±3.59
	***Mfap2*$^{-/-}$**	0.06±0.00	122.40±7.71	55.43±21.47
	***p* value**	0.466	0.121	0.351
CCl_4 (4W)	***Mfap2*$^{+/+}$**	0.04±0.00	121.90±10.36	90.16±2.36
	***Mfap2*$^{-/-}$**	0.04±0.00	108.40±8.53	82.40±2.44
	***p* value**	0.551	0.343	0.052
CCl_4 (8W)	***Mfap2*$^{+/+}$**	0.04±0.00	139.50±1.44	76.01±2.89
	***Mfap2*$^{-/-}$**	0.05±0.00	130.50±5.08	65.79±4.22
	***p* value**	0.277	0.098	0.070

CCl_4 (R4W)	***Mfap2*$^{+/+}$**	0.06±0.01	41.92±18.41	65.02±14.18
	***Mfap2*$^{-/-}$**	0.06±0.00	29.19±6.32	45.78±9.62
	***p* value**	0.796	0.531	0.294
CCl_4 (6W)	**Null**	0.05±0.00	138.50±5.11	122.10±36.54
	ov*Mfap2*	0.04±0.00	131.30±4.27	77.04±1.40
	***p* value**	0.224	0.339	0.285
CCl_4 (R3W)	**Null**	0.06±0.00	13.18±3.10	23.36±1.05
	ov*Mfap2*	0.06±0.00	8.70±1.45	14.20±1.19
	***p* value**	0.837	0.215	0.000
BDL (14D)	***Mfap2*$^{+/+}$**	0.59±0.02	36.27±2.39	31.21±7.56
	***Mfap2*$^{-/-}$**	0.58±0.02	43.43±5.16	31.77±2.47
	***p* value**	0.705	0.243	0.946
BDL (14D)	**Null**	0.65±0.02	32.66±6.25	41.90±7.96
	ov*Mfap2*	0.62±0.03	30.07±7.31	41.47±6.71
	***p* value**	0.413	0.793	0.970

212 LW/BW ratio: liver to body weight ratio.